2024 Tenth Indian Control Conference (ICC)
9 - 11 December, 2024
IISER Bhopal, India

Formation Flying for Fixed Wing UAVs with Obstacle Avoidance through Narrow Gaps

Anish Antony, Shashi Ranjan Kumar, and Dwaipayan Mukherjee

Abstract— **A formation control algorithm based on artificial potential fields for fixed-wing unmanned aerial vehicles to traverse through environments filled with non-cooperative static obstacles is proposed in this paper. The spherical formation is created with a virtual leader at the centre of the sphere and other UAVs positioned on the circumference at a predefined radius. The formation is created using a combination of leader-follower and behavioural formation structure concepts combined with an improved artificial potential field approach. The agents are equipped with obstacle avoidance capabilities through the rotational artificial potential field method. The common issues of local minima entrapment can be avoided with this concept. The paper introduces an algorithm that will empower the formation to travel through narrow passages using dynamic formation reconfiguration. When the obstacles are in close proximity, an algorithm to generate a convex hull of obstacles is also proposed in this work. The efficacy of the proposed algorithms is demonstrated through MATLAB simulations.**

Unmanned aerial vehicles, formation flight, artificial potential field, collision avoidance, obstacle avoidance

I. Introduction

The rapid advancements in computation, sensors, and communication technologies have sparked significant interest among researchers in multi-unmanned aerial vehicle (UAV) formation flying with obstacle avoidance capabilities. In comparison with a single UAV mission, a multi-UAV formation can work cohesively in coordination with each other thereby enabling them to handle complex missions with much smaller budgets and ensuring utmost security [1]. Quick decision making capabilitly along with information exchange and environment perception capability make them ideal for civilian applications (such as smart agriculture and traffic monitoring as well as military applications such as (search and rescue, battlefield surveillance [2]).

In a multi-UAV formation flight, multiple UAVs are generally arranged in the three-dimensional environment in a predefined spatial arrangement with definite architectures for control, sensing and inter-agent communication. Researchers have come up with various formation control architectures such as leader-follower, behavioral structures and virtual structure in literature [3] over the last two decades. Do et al. [4] have provided an excellent survey on various formation control architectures with particular focus on control algorithms, computation, planning, scalability, computation, communication and control architectures.

Obstacle detection and avoidance are of paramount importance in formation flying in ensuring mission safety and reliability. In general, reactive obstacle avoidance strategies can be broadly classified into gap-based methods, potential field methods, geometric methods, optimization methods, and intelligent methods [5]. Artificial potential fields, velocity field histograms, collision cones, and velocity obstacles are some of the popular approaches adopted by researchers in literature [5].

Obstacle avoidance based on artificial potential fields (APF) was first proposed by Khatib in 1986 [6] where a combination of attractive and repulsive potential fields are defined to drive the mobile robots towards the target without collision with an obstacle. Although this approach is easy to implement and computationally less intensive, it suffers from the issue of local minimum entrapment. When the repelling field around the obstacle and the attractive field from the target is directly opposite, it may cancel out and local minimum entrapment can occur [5].

Various researchers have come up with modifications for APF to avoid local minimum entrapment in recent years [7], [8]. One of the approaches proposed by Rezaee et.al. [9] was to use an elliptical repulsive potential field around a rectangular obstacle that can deflect the incoming robots in clockwise/counter-clockwise direction thereby avoiding the issue of getting stuck in a local minimum in 2D. This approach was further extended to 3D by [10] where a leader-follower structure was implemented along with rotational APF to achieve obstacle evasion. The idea of rotational APF in 3D was also used by [11] where an exponential obstacle avoidance function was employed to evade the obstacle.

This paper attempts to extend the work in [11] and proposes two new approaches in tandem with the rotational APF approach for obstacle evasion and formation flying. Formation generation and collision avoidance of agents are achieved using the attractive and repulsive fields and obstacle evasion is achieved using rotational APF. While traversing through narrow gaps, APF-based algorithms traditionally have been found to have certain limitations. The proposed algorithm will help the formation to handle narrow gaps scenarios using formation reconfiguration (compression and expansion). An alternate algorithm is also proposed to address the scenarios where distances between the obstacles are very less (such that the formation can't pass through even with formation reconfiguration).

II. Problem Statement

The primary focus of this work is to develop an algorithm that can enable the formation to traverse through narrow spaces and close areas using the concept of artificial potential fields. The spherical formation described in this paper consists of a virtual UAV at the center of the formation

sphere of radius r_a and four identical agent UAVs spread over the sphere's circumference, maintaining a constant distance from the virtual leader and avoiding collision with obstacles and other member agents. Formation generation and obstacle avoidance is achieved with the help of artificial potential fields. The traditional APF based obstacle avoidance approaches are found to be wanting when presented with scenarios where the formation has to navigate through tight spaces. The paper tries to put forth a comprehensive algorithm that will help the UAV formation to mitigate these issues.

A. UAV Dynamics

It is assumed that the virtual leader and the four agent UAVs that comprise the spherical formation are rigid and have identical dynamics [12]. For the sake of simplicity, only the translational dynamics are considered, and the rotational dynamics of all the agents and the leader are neglected. The 3 degrees of freedom dynamical equation for the point mass model of i^{th} member is given by

$$\dot{V}_i = \frac{T-D}{m} - g\sin\gamma_i \tag{1a}$$

$$\dot{\gamma}_i = \frac{1}{mV}(L\cos\delta_i - mg\cos\gamma_i) \tag{1b}$$

$$\dot{\chi}_i = \frac{L\sin\delta_i}{mV\cos\gamma_i}, \tag{1c}$$

where $D, \chi_i, \gamma_i, V_i, g, m$ represents the drag force, heading angle, flight path angle, air relative velocity, acceleration due to gravity, and mass of i^{th} UAV. The position and velocity coordinates in the inertial coordinate frame are given by $\mathbf{r}_\mathrm{i} = [x_i, y_i, z_i]^T$ and $v_i = \dot{\mathbf{r}}_\mathrm{i} = [\dot{x}_\mathrm{i}, \dot{y}_\mathrm{i}, \dot{z}_\mathrm{i}]^T$ respectively. Thrust T, bank angle δ_i and lift force L are the control input vectors of the UAV. The dynamics of UAV position coordinates are given by $\dot{x}_i = V_i\cos\gamma_i\cos\chi_i$, $\dot{y}_i = V_i\cos\gamma_i\sin\chi_i$, $\dot{z}_i = V_i\sin\gamma_i$ Feedback linearization is employed [13] and virtual input

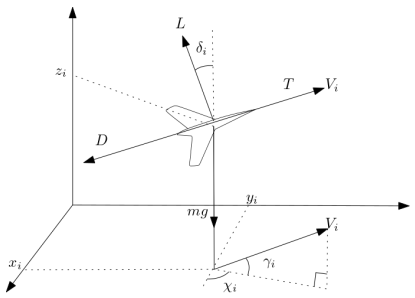


Fig. 1: UAV model in inertial coordinate frame [11].

accelerations $\left(U_i = [U_{x_i}, U_{y_i}, U_{z_i}]^T\right)$ in inertial frame.

$$\ddot{x}_i = U_{x_i}, \quad \ddot{y}_i = U_{y_i}, \quad \ddot{z}_i = U_{z_i}, \tag{2}$$

The proposed algorithm is utilized to generate the virtual acceleration commands in x, y, and z directions of the inertial frame, and the real UAV control inputs,$(T, \delta_i L)$, can be computed as:

$$\delta_i = \tan^{-1}\left[\frac{U_{y_i}\cos\chi_i - U_{x_i}\sin\chi_i}{(U_{z_i}+g)\cos\gamma_i - (U_{x_i}\cos\chi_i + U_{y_i}\sin\chi_i)\sin\gamma_i}\right] \tag{3a}$$

$$L = \frac{m\left((U_{z_i}+g)\cos\gamma_i - (U_{x_i}\cos\chi_i + U_{y_i}\sin\chi_i)\sin\gamma_i\right)}{\cos\delta_i} \tag{3b}$$

$$T = m\left((U_{z_i}+g)\sin\gamma_i + (U_{x_i}\cos\chi_i + U_{y_i}\sin\chi_i)\cos\gamma_i\right) + D \tag{3c}$$

It is assumed that the interagent communication is not disturbed within a certain range and all the agents and virtual leader are equipped with sensors that will enable them to detect the presence of targets, obstacles, and other agents within a specified range.

III. Formation generation, obstacle avoidance and narrow gap traversal

The overall work can be grouped into three stages: formation generation and maintenance, obstacle avoidance using rotational potential fields, and narrow gap traversal using formation reconfiguration. The first two stages have been described in detail in [11]. This paper primarily focuses on the narrow gap traversal of the formation by formation reconfiguration or by obstacle avoidance of a convex hull of close by obstacles .

A. Formation Generation

The formation works in a leader-follower formation control system, wherein the formation trajectory is generated by the virtual leader depending upon the position of the target that is sensed using a visual sensor. The agents track the leader's trajectory maintaining a predefined distance.

The tracking potential of the virtual leader $V_{\text{tracking,VL}}$ as given by [14]

$$V_{\text{tracking,VL}} = K_{1_{\text{VL}}}||\mathbf{r}_{\text{VL}} - \mathbf{r}_{\text{tar}}|| + \frac{1}{2}K_{2_{\text{VL}}}\dot{\mathbf{r}}_{\text{VL}}^T.\dot{\mathbf{r}}_{\text{VL}}, \tag{4}$$

Target's position vector and virtual leader's position and velocity vectors are denoted by $\mathbf{r}_{\text{tar}} = [x_{\text{tar}}, y_{\text{tar}}, z_{\text{tar}}]^T$, $\mathbf{r}_{\text{VL}} = [x_{\text{VL}}, y_{\text{VL}}, z_{\text{VL}}]^T$, and $\dot{\mathbf{r}}_{\text{VL}} = [\dot{x}_{\text{VL}}, \dot{y}_{\text{VL}}, \dot{z}_{\text{VL}}]^T$ respectively. Tracking error and transient behaviour is dictated by the choice of constants $K_{1_{\text{VL}}}$ and $K_{2_{\text{VL}}}$

The formation is generated using the attractive and repulsive potential fields that are constructed around the leader and agents as given in [11]. Attractive and repulsive forces which are created in the direction of minimizing potential around each agent, act in tandem to drive the agents to a spherical formation. The total force on each agent is the sum of attractive and repulsive forces acting on it. Attractive forces towards the virtual leader at the center of the sphere help in maintaining the spherical shape of the formation. The repulsive forces generated by other agents as well as obstacles help in evading cooperative as well as non-cooperative obstacles.

The attractive formation potential, $V_{\text{att,i}}$ that drives i^{th} agent towards the formation sphere and the repulsive formation

potential, $V_{\text{rep,i}}$, that avoids interagent collisions can be defined as ([9], [11]),

$$V_{\text{att,i}} = \frac{K_{1_{\text{att}}}}{4}\left((\mathbf{r}_\text{i} - \mathbf{r}_\text{VL})^T \cdot (\mathbf{r}_\text{i} - \mathbf{r}_\text{VL}) - r_\text{a}^2\right)^2 + \frac{K_{2_{\text{att}}}}{2}\dot{\mathbf{r}}_\text{i}^T.\dot{\mathbf{r}}_\text{i} \tag{5a}$$

$$V_{\text{rep,i}} = K_{1_{\text{rep}}} q_\text{i} \sum_{j=1, j\neq i}^{4} q_\text{j} \sqrt{\frac{1}{\mathbf{r}_\text{ij}^T.\mathbf{r}_\text{ij}}} \tag{5b}$$

The spherical formation convergence depends on the choice of the attractive potential gains, $K_{1_{\text{att}}}$ and $K_{2_{\text{att}}}$ and repulsive potential gain, $K_{1_{\text{rep}}}$. The repulsive potential field is analogous to Coulomb's potential among the electric charges. All the member UAVs are assumed to have the same electric charge (q_j) to generate a repulsive potential as the interagent distance reduces. The formation potential of i^{th} UAV will be a combination of attractive and repulsive potential functions, $V_{\text{form,i}} = V_{\text{att,i}} + V_{\text{rep,i}}$. Leader and member potential functions can be combined to generate total formation potential function, $V_{\text{tot}} = V_{\text{tracking,VL}} + \sum_{i=1}^{4} V_{\text{form,i}}$. The desired formation generation force of i^{th} member UAV can be computed by taking the negative gradient of the member potential function,

$$F_\text{i} = -\frac{1}{K_{2_{\text{att}}}}(\nabla V_{\text{att,i}} + 2\nabla V_{\text{rep,i}} + K_{\text{v1}}\dot{\mathbf{r}}_\text{i}) \tag{6}$$

The force on the virtual leader is given as,

$$F_\text{VL} = \frac{-1}{K_{2_\text{VL}}}\left[K_{1_\text{VL}}\frac{(\mathbf{r}_\text{VL} - \mathbf{r}_\text{tar})}{||\mathbf{r}_\text{VL} - \mathbf{r}_\text{tar}||} - \sum_{i=1}^{4}\nabla V_{\text{att,i}} + K_{\text{v2}}\dot{\mathbf{r}}_\text{VL}\right] \tag{7}$$

Formation flying control law for each member UAV can be computed as, $U_\text{i} = \frac{F_\text{i}}{m}$, where m is the member UAV mass, $U_i = [U_{x_i}, U_{y_i}, U_{z_i}]^T$, $F_i = [F_{x_i}, F_{y_i}, F_{z_i}]^T$, $\forall\ i = 1,2,3,4$.

B. Obstacle avoidance using rotational potential fields

Obstacle avoidance using the concept of rotational artificial potential fields was introduced by Rezaee et.al. [9] in order to avoid local minimum entrapment. The idea was further enhanced to 3D by Chang et.al [15] but suffers from certain limitations. An exponential obstacle avoidance force based on rotating potential field concept was proposed by [11], wherein a rotational potential field was created around a cuboid obstacle with dimensions $(2l_{\text{o1}}, 2b_{\text{o1}}, 2h_{\text{o1}})$, centered at $r_{\text{o1}} = (x_{\text{o1}}, y_{\text{o1}}, z_{\text{o1}})$ (parallel to x, y and z axis) in [11]. The rotational potential fields are ellipsoidal and the strength of the field decreases as the distance of the UAV away from the obstacle increases. The formation control law for i^{th} UAV,

$$U_\text{i} = \frac{F_\text{i} + F_{\text{OAi}}}{m} \tag{8}$$

The repulsive rotational potential field around the cuboid obstacle will be active only when the UAV is within the sphere of influence of the obstacle,

$$(r_{io1} - [\lambda_1(\max(l_{o1}, b_{o1}, h_{o1}))]) <= 0 \tag{9}$$

The distance between the UAV and obstacle center is denoted by $r_{io1} = |r - r_{1OA}|$ and λ_1 is the obstacle gain detection factor.

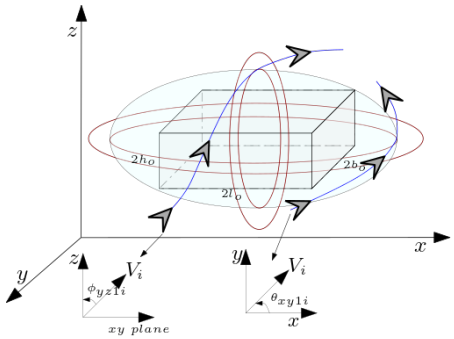


Fig. 2: Rotational potential fields around an obstacle [11].

The rotational potential field around the obstacle can be either parallel to the $x-y$ (horizontal) plane or parallel to $y-z$ (vertical)plane. When the horizontal plane is activated, either a clockwise field or a counterclockwise field will be generated depending upon criteria computed using certain angles. Similarly, when the vertical plane is selected for obstacle evasion, either an upward or downward field is selected based on the angle criteria. The type of rotational potential field selected for obstacle avoidance depends upon three angles, [11]: the angle between the $x-y$ plane and UAV velocity vector,θ_{xy1i}, the angle between the vector joining UAV position with obstacle center position and x-axis,θ_{xy2i}, and the angle between tangent direction of potential field and x-axis,θ_{xy3i}. The analogous angles in $y-z$ plane are denoted by ϕ_{yz1i},ϕ_{yz2i} and ϕ_{yz3i}. The rotational potential field selection criteria and the details of the magnitude of the obstacle avoidance potential, as well as the resulting actuation forces for both planes, are given in detail in [11]. The complete obstacle avoidance force for evading the obstacle can be computed as

$$F_{\text{OAi}} = \frac{f_{\text{OAi}}}{|f_{\text{OAi}}|}K_{o1}e^{-K_{o2}r_{io1}} \tag{10}$$

Obstacle gain parameters,K_{o1}, K_{o2} and K_{o3}, help in modifying the amplitude of the repulsive force depending upon the UAV's distance from the obstacle and size of the obstacle, $(K_{o1} = K_{o3}(l_{o1}b_{o1}h_{o1}))$. The direction of the motion of the UAV around the obstacle depends on the chosen rotational field and the resulting exponential obstacle avoidance force, f_{OAi}, as detailed in [11] (one among f_{ixycl}, f_{ixyccl}, f_{iyzup} and $f_{iyzdown}$ will be selected when the UAV enters the sphere of influence of the obstacle).

C. Obstacle avoidance for closely placed obstacles

The traditional approach of obstacle avoidance(OA) based on APF [6] has certain limitations while traversing through narrow gaps between closely placed obstacles. While encountering an obstacle, the agents take a detour and rejoin the original trajectory after moving away from the obstacle using the classical obstacle avoidance concept. Even when two obstacles are placed gap in between, the formation will take a large detour to avoid both obstacles. The detour will demand a certain amount of control effort which might eat into the fuel budget earmarked for other activities.

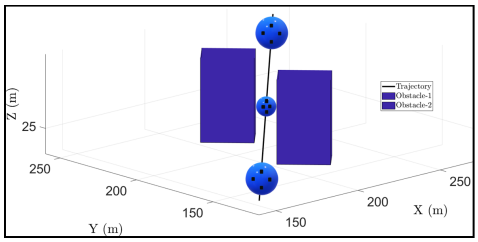


Fig. 3: Illustration of formation compression and expansion.

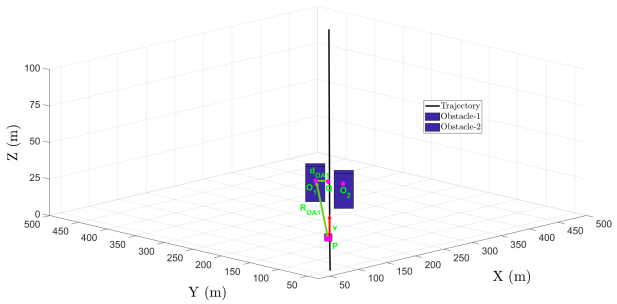


Fig. 4: Formation compression/expansion activation algorithm.

In this section, two innovative approaches to encounter multiple obstacle scenarios are considered. One approach to traverse through the narrow gaps between obstacles is to alter the formation shape. The spherical formation considered in this study can shrink and expand to a certain spherical formation radius depending upon the requirements. Another approach to obstacle evasion in scenarios where multiple obstacles are placed in close proximity in such a way that the formation traversal is infeasible even after formation reconfiguration , a convex hull encompassing all the obstacles is created and obstacle evasion using rotational APF is activated.

1) Formation compression and expansion: The obstacle avoidance algorithm guides the formation to take a detour, avoiding both obstacles. However, if the gap between the obstacles is larger than the minimum possible formation radius, the formation can pass through the gap without triggering the obstacle avoidance manoeuvre.

When the formation encounters a narrow gap, the formation has two options: it can either take a detour using an obstacle avoidance algorithm or temporarily compress its shape to pass through the gap and then expand back to its original configuration. The formation can increase and decrease the formation radius within specified values by adjusting the initialization values,r_a, in 5a. The idea of spherical formation compressing to a lower radius upon encountering a narrow gap and then expanding back to the original shape after passing the gap is illustrated in Fig. 3.

2) Algorithm to activate formation compression/expansion: Considering the formation's potential to expand and contract in a finite time, an important consideration arises as to how to activate the formation compression and expansion algorithm in the presence of multiple obstacles.

Two cuboid-shaped static obstacles placed with a narrow gap between them are illustrated in Fig. 4. For the formation to pass through the gap without collision (illustrated in Fig. 3), the minimum gap between the obstacles should be at least larger than the minimum possible formation radius.

Let $\bar{v}_{VL}$ be the velocity of the virtual leader at a particular point P, which is at a distance of R_{OA1} from the obstacle O_1 in Fig. 4. Assuming that the leader maintains its current velocity, the minimum distance of the obstacle center, O_1, from the trajectory, d_{OA1} is computed as

$$d_{OA1} = R_{OA1} \sin\left(\cos^{-1}\frac{\bar{R}_{OA1}\cdot\bar{v}_{VL}}{||\bar{R}_{OA1}||\cdot||\bar{v}_{VL}||}\right) \tag{11}$$

The distance of the leader from the obstacle center O_2, d_{OA2}, can also be computed in similar manner. The formation compression algorithm can be activated if both the distances d_{OA1} and d_{OA2} are greater than the minimum possible formation radius with a certain specified tolerance. The formation expansion algorithm can be activated to bring the formation back to its original shape after the formation has crossed both obstacles.

3) Obstacle avoidance using convex hull concept: A potential scenario that the formation is likely to encounter is multiple obstacles placed with very small distance between them such that the formation may not be able to pass through it even with formation reconfiguration. This section puts forth another strategy that can be adopted in such scenarios. When the formation enters the obstacle's sphere of influence, the relative distances between the obstacle centers can be computed. If the distances between obstacles are below a specified threshold, the strategy is to consolidate these obstacles and consider them as a single, larger obstacle. In other words, a convex hull containing all smaller obstacles can be computed.

It has to be noted that the static obstacles considered here are either cuboid in shape or can be encompassed in a cuboid(placed parallel to the x,y, and z axis). The convex hull of obstacles is created by computing the maximum and minimum values in all three directions. $x_{\mathrm{OA}_{max}} = \max(x_{OA1}, x_{OA2}, x_{OA3})$, $x_{\mathrm{OA}_{min}} = \min(x_{OA1}, x_{OA2}, x_{OA3})$. Computation of $y_{\mathrm{OA}_{max}}, y_{\mathrm{OA}_{min}}, z_{\mathrm{OA}_{max}}$ and $z_{\mathrm{OA}_{min}}$ can be carried out in a similar manner. Center of the convex hull of obstacles can be computed as

$$[x_{OAch},\ y_{OAch},\ z_{OAch}] = \left[\frac{x_{\mathrm{OA}_{max}}+x_{\mathrm{OA}_{min}}}{2}, \frac{y_{\mathrm{OA}_{max}}+y_{\mathrm{OA}_{min}}}{2}, \frac{z_{\mathrm{OA}_{max}}+z_{\mathrm{OA}_{min}}}{2}\right] \tag{12}$$

The dimensions of the big obstacle, $(2l_{OAch},\ 2b_{OAch},\ 2h_{OAch})$ can be computed by $(l_{OAch},\ b_{OAch},\ h_{OAch}) = \left(\frac{|x_{\mathrm{OA}_{max}}-x_{\mathrm{OA}_{min}}|}{2}, \frac{|y_{\mathrm{OA}_{max}}-y_{\mathrm{OA}_{min}}|}{2}|, \frac{|z_{\mathrm{OA}_{max}}-z_{\mathrm{OA}_{min}}|}{2}\right)$. Once the convex hull of obstacles is created, then the rotational obstacle potential field will be used to evade it considering it as a single large obstacle.

4) Combined Algorithm: When multiple obstacles are present, the proposed formation reconfiguration and convex hull obstacle creation algorithms need to work in tandem to achieve the best performance. The proposed algorithms are combined into a single one as depicted in 1.

Algorithm 1: Obstacle avoidance (OA) algorithm to traverse through narrow gaps

Input : States of agents,leader and obstacle
Output: Final acceleration commands to UAVs

```
Initiate formation generation using APF
Initiate target tracking by virtual leader using APF
if ( Obstacles present in the sphere of influence?) then
    if ( Multiple obstacles present?) then
        /* Check for formation reconfiguration */
        if ( Obstacles lie in the future trajectory?) and (gap available for formation to traverse?) then
            Initiate formation compression and expansion
        else
        /* Check if obstacles are close enough to create a convex hull */
            Compute distance between obstacles
            if (Gap between selected obstacles lesser than threshold?) then
                Create convex hull of obstacles
                Activate OA using rotational APF for the convex hull
            else
                Activate OA using rotational APF
    else
        Activate OA using rotational APF for single obstacle
Compute the desired formation control and obstacle avoidance forces and acceleration
```

IV. Simulations

The efficacy of the proposed algorithms in an obstacle-laden 3D environment is demonstrated using numerical simulations in MATLAB. Consider a mobile target initially located at $(30,20,10)$ and traverses with an acceleration of $a_{tx} = 1$ m/s^2, $a_{ty} = 1\sin(1/8.t)$ m/s^2, and $a_{tz} = 0.5$ m/s^2. The virtual leader is initially positioned at origin $(-1,-1,-1)$ and member UAVs at $(0.1,1,2.5)$, $(3.5,3.5,7)$, $(2,-1,6.5)$, $(2,3,6.5)$ respectively. The formation radius is set at 4 m. Two static cuboid obstacles centered at $(200,180,34)$ and at $(250,230,44)$ with dimensions of $l_o1 = 8$ m, $b_o1 = 12$ m and $h_o1 = 12$ m and $l_o2 = 4$ m, $b_o2 = 6$ m and $h_o2 = 6$ m respectively. The formation trajectory in the presence of two cuboid obstacles is depicted in Fig. 5a. The cyan-coloured spheres in the figure indicate the formation spheres at discrete instants of time.

The member UAVs converge to the surface of the formation sphere quickly and maintain the formation as shown in Fig. 5b. The formation gets disturbed while evading the obstacle and regroups back into its original shape after evading the obstacle with a sufficient gap from the obstacle as shown in Fig. 5c

Obstacle avoidance of the UAV formation using rotational potential field concept while encountering two closely placed obstacles of identical size, $(8\times12\times12)$, positioned at $(200,197,34)$ and $(200,163,34)$ respectively (gap of ≈ 10m between closest obstacle surfaces) is demonstrated in Fig.6a. Even though the agent maintains a sufficient gap from the obstacle center, the formation takes a large detour from the original trajectory.

The same simulation when repeated using the proposed formation compression expansion concept, the formation reconfiguration is initiated as the gap between the obstacles is greater than the formation radius. The formation compresses to a smaller sphere of radius and then expands back to its original shape after crossing the obstacle. The UAV formation passes through the narrow gap between the obstacles without initiating the obstacle avoidance manoeuvre as shown in Fig. 6b. The variation in formation radius during the process of formation motion as evident from Fig. 6c, indicates the shrinking and expansion of the formation sphere while traversing in the narrow obstacle gap.

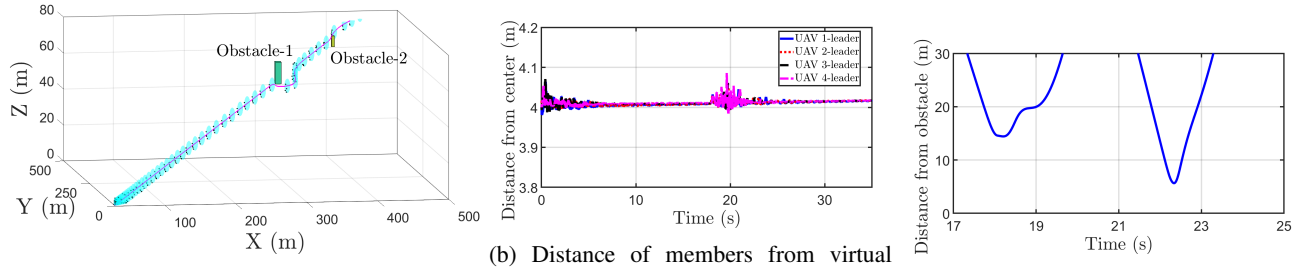
When the obstacles are placed with gaps lesser than the formation radius with a predefined tolerance, obstacle avoidance using rotational APF results in a collision as shown in Fig. 7a. In such scenarios, a convex hull of obstacles can be created and obstacle avoidance using rotational APF can be initiated as shown in Fig. 7b and Fig. 7c .

V. Conclusion

The strategies for formation motion through narrow gaps are developed in this paper. A spherical UAV formation with a virtual leader at the center and member UAVs spread around the circumference of the virtual sphere is generated using APF. A reactive obstacle avoidance strategy based on rotational APF is combined with the formation APF to ensure a collision-free formation motion in a static obstacle-laden 3D environment. A novel strategy to improvise this concept while traversing through narrow gaps using formation reconfiguration (compression and shrinking) is also proposed. An algorithm to create and evade a convex hull of small obstacles using rotational APF is also proposed in this paper. The performance of the proposed concepts is demonstrated through MATLAB simulations.

VI. Acknowledgements

This work was supported in part by the Ministry of Electronics and Information Technology, India, via Capacity building for Human Resource Development in Unmanned Aircraft Systems (Drone and related technology) - Guidance, Navigation, and Control Algorithms and Simulations (Reference No: L-14011/29/2021-HRD).

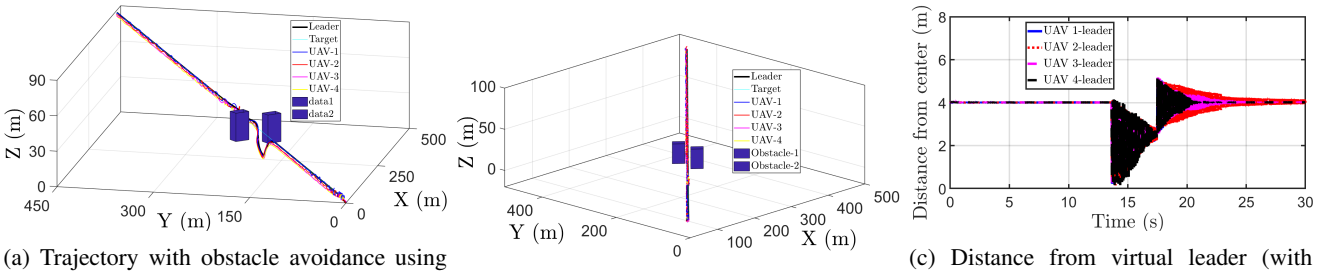


(a) Formation trajectory with obstacle avoidance leader

(b) Distance of members from virtual

(c) Distance of agents from obstacles

Fig. 5: Formation flying of four UAVs with obstacle avoidance.

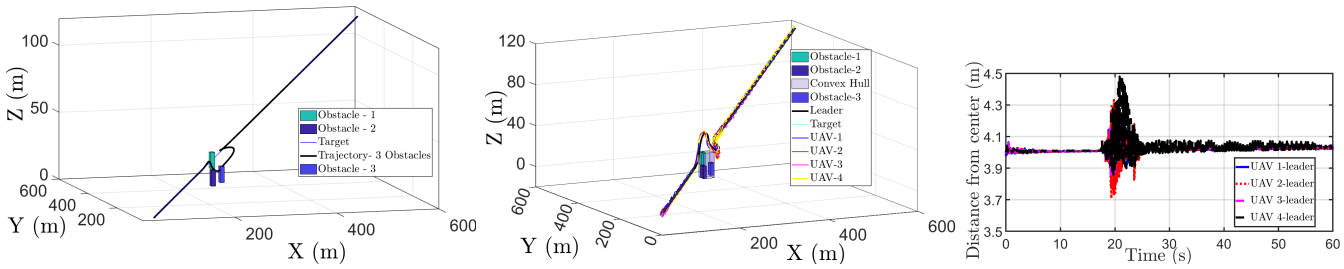


(a) Trajectory with obstacle avoidance using rotational APF

(b) Trajectory with formation reconfiguration

(c) Distance from virtual leader (with formation reconfiguration)

Fig. 6: Formation trajectory with reconfiguration (compression and expansion) while encountering narrow gaps.



(a) Trajectory with rotational APF

(b) Trajectory after creating a convex hull

(c) Distance of agents from leader

Fig. 7: Obstacle avoidance by creating a convex hull of obstacles and activating rotational APF.

REFERENCES

[1] Z. Zhen, G. Tao, Y. Xu, and G. Song, "Multivariable adaptive control based consensus flight control system for uavs formation," *Aerospace Science and Technology*, vol. 93, p. 105336, 2019.

[2] S. Shao, Y. Peng, C. He, and Y. Du, "Efficient path planning for uav formation via comprehensively improved particle swarm optimization," *ISA transactions*, vol. 97, pp. 415–430, 2020.

[3] Y. Q. Chen and Z. Wang, "Formation control: a review and a new consideration," in *2005 IEEE/RSJ International conference on intelligent robots and systems*. IEEE, 2005, pp. 3181–3186.

[4] H. T. Do, H. T. Hua, M. T. Nguyen, C. V. Nguyen, H. T. Nguyen, H. T. Nguyen, and N. T. Nguyen, "Formation control algorithms for multiple-uavs: A comprehensive survey," *EAI Endorsed Transactions on Industrial Networks and Intelligent Systems*, vol. 8, no. 27, 6 2021.

[5] M. Z. Butt, N. Nasir, and R. B. A. Rashid, "A review of perception sensors, techniques, and hardware architectures for autonomous low-altitude uavs in non-cooperative local obstacle avoidance," *Robotics and Autonomous Systems*, vol. 173, p. 104629, 2024.

[6] O. Khatib, "Real-time obstacle avoidance for manipulators and mobile robots," *The international journal of robotics research*, vol. 5, no. 1, pp. 90–98, 1986.

[7] D. Choi, K. Lee, and D. Kim, "Enhanced potential field-based collision avoidance for unmanned aerial vehicles in a dynamic environment," in *AIAA scitech 2020 forum*, 2020, p. 0487.

[8] E. L. de Angelis, F. Giulietti, and G. Rossetti, "Multirotor aircraft formation flight control with collision avoidance capability," *Aerospace Science and Technology*, vol. 77, pp. 733–741, 2018.

[9] H. Rezaee and F. Abdollahi, "A decentralized cooperative control scheme with obstacle avoidance for a team of mobile robots," *IEEE Transactions on Industrial Electronics*, vol. 61, no. 1, pp. 347–354, 2013.

[10] J. Zhang, J. Yan, and P. Zhang, "Fixed-wing uav formation control design with collision avoidance based on an improved artificial potential field," *IEEE Access*, vol. 6, pp. 78 342–78 351, 2018.

[11] A. Antony, S. R. Kumar, and D. Mukherjee, "Artificial potential fields based formation control for fixed wing uavs with obstacle avoidance," *IFAC-PapersOnLine*, vol. 57, pp. 19–24, 2024.

[12] J. Wang and M. Xin, "Integrated optimal formation control of multiple unmanned aerial vehicles," *IEEE Transactions on Control Systems Technology*, vol. 21, no. 5, pp. 1731–1744, 2012.

[13] P. K. Menon, G. D. Sweriduk, and B. Sridhar, "Optimal strategies for free-flight air traffic conflict resolution," *Journal of Guidance, Control, and Dynamics*, vol. 22, no. 2, pp. 202–211, 1999.

[14] A. Badawy and C. R. McInnes, "On-orbit assembly using superquadric potential fields," *Journal of Guidance, Control, and Dynamics*, vol. 31, no. 1, pp. 30–43, 2008.

[15] K. Chang, Y. Xia, and K. Huang, "Uav formation control design with obstacle avoidance in dynamic three-dimensional environment," *SpringerPlus*, vol. 5, no. 1, pp. 1–16, 2016.